Overlap properties of clouds generated by a cloud-resolving model

L. Oreopoulos

Joint Center for Earth Systems Technology, University of Maryland Baltimore County, Baltimore, Maryland, USA

Laboratory for Atmospheres, NASA Goddard Space Flight Center, Greenbelt, Maryland, USA

M. Khairoutdinov

Department of Atmospheric Sciences, Colorado State University, Fort Collins, Colorado, USA

Received 18 December 2002; revised 17 March 2003; accepted 18 April 2003; published 14 August 2003.

[1] The overlap properties of ~850 snapshots of convective cloud fields generated by a cloud-resolving model are studied and compared with previously published results based on cloud radar observations. Total cloud cover is overestimated by the random overlap assumption but underestimated by the maximum overlap assumption and two standard implementations of the combined maximum/random overlap assumption. When the overlap of two layers is examined as a function of vertical separation distance, the value of the parameter α measuring the relative weight of maximum ($\alpha = 1$) and random ($\alpha = 0$) overlap decreases in such a way that only layers less than 1 km apart can be considered maximally overlapped, while layers more than 5 km apart are essentially randomly overlapped. The decrease of α with separation distance Δz is best expressed by a power law, which may not, however, be suitable for parameterization purposes. The more physically appropriate exponential function has slightly smaller goodness of fit overall but still gives very good fits for Δz between 0 and 5 km, which is the range of separation distances that would be of most importance in any overlap parameterization for radiative transfer purposes. *INDEX TERMS:* 0320 Atmospheric Composition and Structure: Cloud physics and chemistry; 1655 Global Change: Water cycles (1836); 3337 Meteorology and Atmospheric Dynamics: Numerical modeling and data assimilation; 3359 Meteorology and Atmospheric Dynamics: Radiative processes; *KEYWORDS:* clouds, radiative transfer, overlap, cloud-resolving models, general circulation models, cloud parameterization

Citation: Oreopoulos, L., and M. Khairoutdinov, Overlap properties of clouds generated by a cloud-resolving model, *J. Geophys. Res.*, *108*(D15), 4479, doi:10.1029/2002JD003329, 2003.

1. Introduction

[2] One of the main requirements for good performance of radiative transfer algorithms in large-scale models (LSMs) is availability of accurate vertical distributions of cloud fraction [e.g., *Barker et al.*, 1999a]. This is, of course, not an easy requirement to meet, since processes relevant to cloud formation that determine cloud area at different levels of the atmosphere are often of subgrid nature and need to be parameterized. Although it is generally accepted that recent progress with prognostic cloud schemes has resulted in improved LSM cloudiness, evaluating the realism of modeled vertical cloud distributions is still a challenging task. Moreover, even if LSM cloud profiles are realistic, it is still doubtful whether current operational radiative transfer schemes can incorporate this information in a robust way.

[3] One of the most popular assumptions currently used in LSMs is that adjacent cloud layers overlap maximally while cloud layers separated by clear skies overlap randomly. This is based on a compilation of 15-level US Air Force 3D Nephanalysis data by *Tian and Curry* [1989]. To evaluate the degree of cloud profile realism in LSMs, one needs, however, comparisons with more detailed observations. Unfortunately, there is no such global data set available to this day. In the future, the space-based 94 GHz radar instrument CloudSat [*Stephens et al.*, 2002], scheduled for launch in 2004 will hopefully help in filling this observational gap. However, until CloudSat data become available, the best observations of cloud overlap will be ground-based and will be coming from millimeter cloud radar (MMCR) operating at few selected sites.

[4] Ground-based radar data have already been used for studies of cloud overlap: *Hogan and Illingworth* [2000] (hereinafter referred to as HI2000) derived overlap statistics (discussed later) from radar observations in southern England for the period November 1998 to January 1999. *Mace and Benson-Troth* [2002] (hereinafter referred to as MBT2002) performed similar analysis using a much more extensive data set that included 103 months of MMCR observations at three (tropical, midlatitude, and polar) sites of the Atmospheric Radiation Measurements (ARM) program, and were thus able to examine seasonal cycles in overlap and differences among climate regimes. *Hogan and Illingworth* [2003] used MMCR data to study the overlap characteristics of the in-cloud fluctuations of water content.

0148-0227/03/2002JD003329

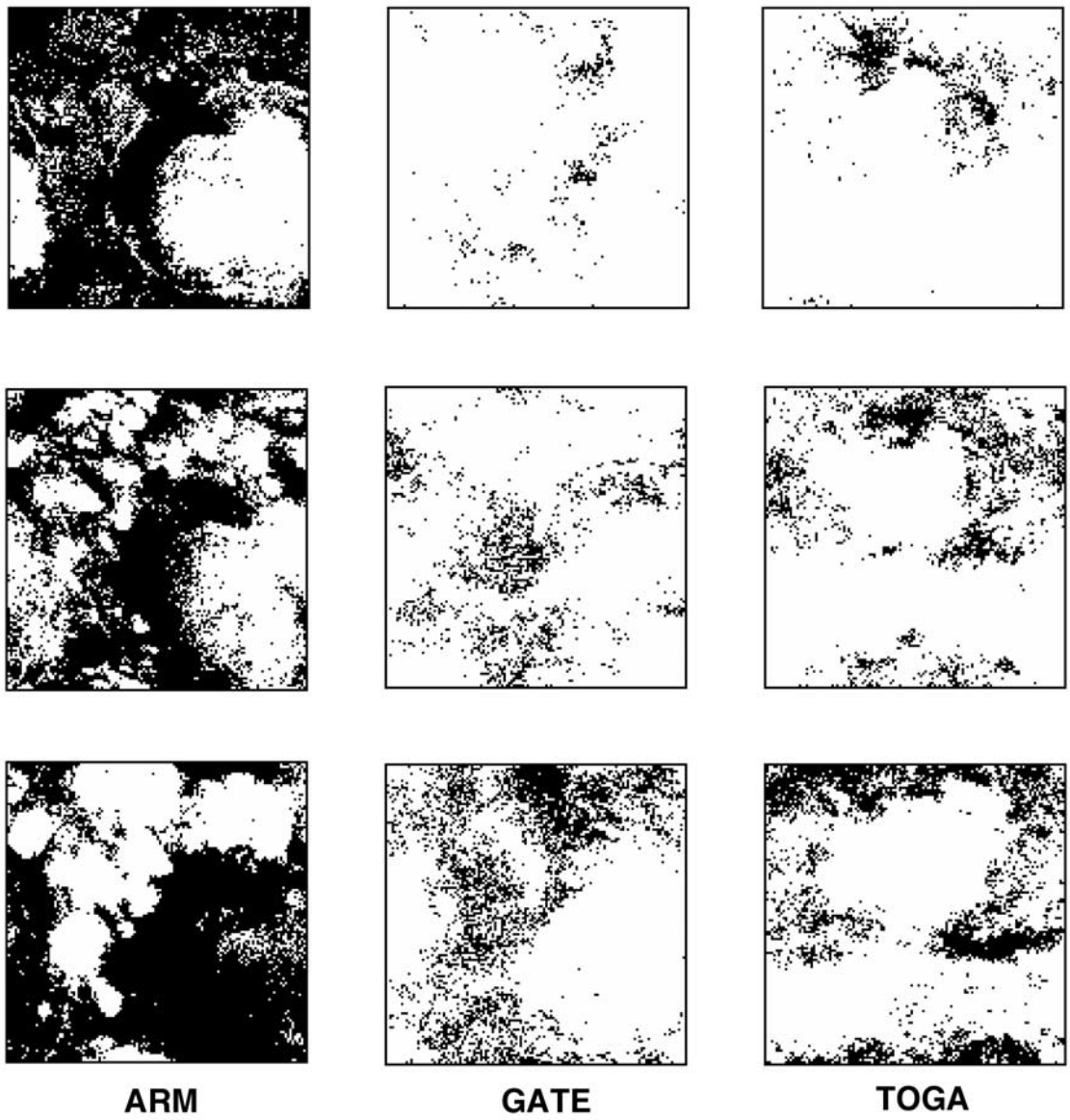

Figure 1. Cloud masks (black is clear and white is cloudy sky) of three randomly selected consecutive snapshots from each experiment showing the fast decorrelation of the cloud fields.

[5] In this paper we use a different type of data set to study cloud fraction overlap: cloud fields from a cloud-resolving model (CRM). Cloud fields from CRMs have recently become quite popular inputs for testing atmospheric radiative transfer algorithms [*Oreopoulos and Barker*, 1999; *Barker et al.*, 1999a, 2003; R. Scheirer and A. Macke, Cloud inhomogeneity and broadband solar fluxes, submitted to *Journal of Geophysical Research*, 2002]. The rationale behind their use in this context is that they provide instantaneous full 3-D "snapshots" of cloud fields with well-defined spatial scales, which are considered quite realistic representation of actual cloud fields. In this work, we proceed then with the assumption that the realism of CRM cloud fields makes them a good source of useful statistical information on cloud vertical overlap. It should be pointed out, however, that our results can probably be considered typical of only the three regions of the globe whose convective cloud fields the CRM attempts to simulate. As with the MMCR studies, these regions may have their local biases and the results may not be automatically applicable to a wider range of geographical locations and meteorological conditions. They are also specific to the vertical bin size (0.5 km) and domain size ($\sim$250 and $\sim$500 km) of our analysis and the horizontal resolution (2 km) of the data set.

2. Data Set

[6] A detailed description of the CRM used in this study is given by *Khairoutdinov and Randall* [2003]. The convective cloud fields come from runs using the time varying forcing derived from observations collected during intensive observation periods (IOPs) of ARM, GATE (Global Atmospheric Research Program (GARP) Atlantic Tropical

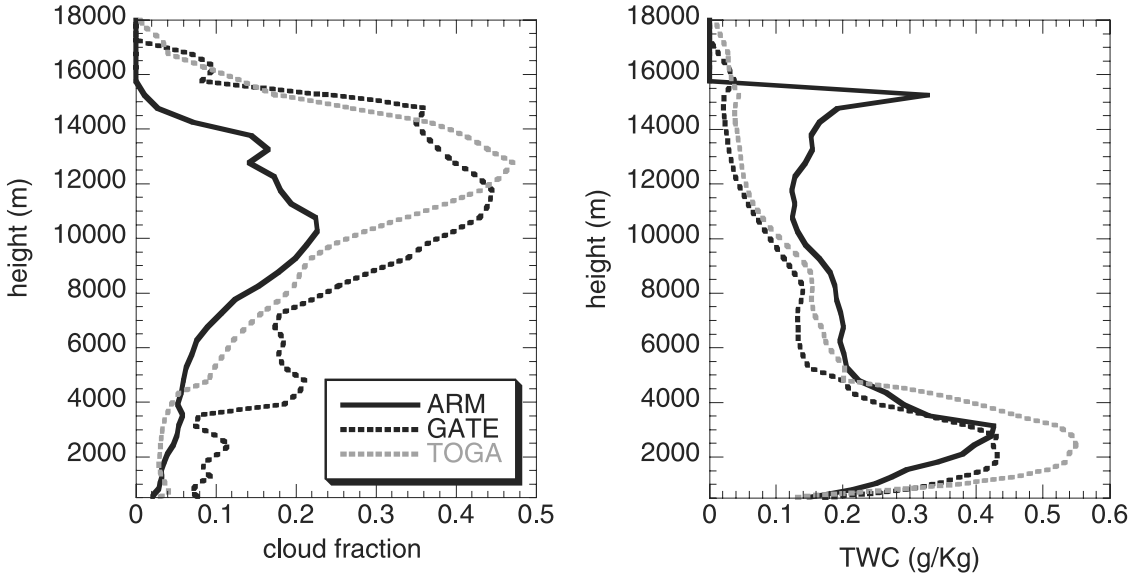

Figure 2. Ensemble average profiles of cloud fraction and total (nonprecipitating) water content TWC for the simulated ARM, GATE, and TOGA cloud fields used in this study.

Experiment), and TOGA-COARE (Tropical Ocean and Global Atmosphere Coupled Ocean-Atmosphere Response Experiment). The ARM forcing is from the Summer 1997 IOP over Oklahoma and Nebraska from 18 June to 16 July [*Khairoutdinov and Randall*, 2003]; the GATE Phase III forcing covers the period from 1 to 18 September 1974; finally, the TOGA-COARE (hereinafter, for brevity, "TOGA") data set corresponds to the time period from 18 December 1992 to 8 January 1993. For all three cases, the domain size is 512 km × 512 km with 2 km horizontal grid size and variable vertical resolution: ~100–200 m up to the first two kilometers, gradually increasing to 500 m at a height of ~6 km. The number of fields with significant cloud amount for statistical analysis is 193 for ARM, 164 for GATE, and 498 for TOGA and are "snapshots" saved every hour. We found that this time interval is sufficient for significant decorrelation and thus relatively high degree of independence of the cloud fields. Since it is extremely difficult to determine decorrelation quantitatively in our case, we demonstrate it empirically by showing in Figure 1 cloud masks (from total cloud cover calculations explained later) of three randomly selected successive snapshots from each experiment. Figure 1 shows that the cloud fields are changing fast. This is consistent with the lifetime of convective cloud cells being usually less than an hour and the presence of wind shear which drives existing cells further apart.

[7] In order to study overlap also for domain sizes closer to those of typical General Circulation Models, we split the domain into four $(256\text{km})^2$ subdomains, and performed additional analysis. Many results are shown for both domain sizes. We did not attempt to examine in detail overlap dependence on domain size by splitting into even smaller subdomains because the relatively coarse resolution of 2 km and the rather small layer cloud fractions in many fields yields relatively few cloudy grid points for small subdomains and thus more noisy results per snapshot.

[8] For each model layer the cloud fraction is determined by counting the number of grid boxes with nonprecipitating total water (liquid and ice) greater that 10^{-5} g/Kg. Figure 2 shows cloud fraction and TWC profiles derived by ensemble-averaging individual cloud fields. GATE fields have larger cloud fractions than the ARM and TOGA fields, except for high altitudes where TOGA has slightly more clouds. TOGA has the highest TWC at low altitudes (<4 km) where the cloud fractions are very low, and ARM the highest above that altitude. Even though no layer of the GATE and TOGA data set has ensemble-average cloud fraction above 0.5, the total cloud cover (fraction of columns with at least one cloudy grid box) is much higher (mean values of "true" curve in Figure 3, middle and bottom), and frequently assumes values corresponding to overcast conditions.

3. Overlap Analysis

[9] The large number of cloud fields from the CRM runs gives us some assurance that meaningful statistics of cloud overlap characteristics can be obtained. As we go through the presentation of our results, we will be providing information on how to calculate cloud fractions from the various overlap assumptions. We start immediately below with three classic overlap assumptions. Given two cloud layers, their combined cloud fraction, when only their individual cloud fractions C_1 and C_2 are known, can be calculated from (e.g., MBT2002):

$$C_{\max} = \max(C_1, C_2) \tag{1a}$$

$$C_{\min} = \max(1, C_1 + C_2) \tag{1b}$$

$$C_{\text{ran}} = C_1 + C_2 - C_1 C_2 \tag{1c}$$

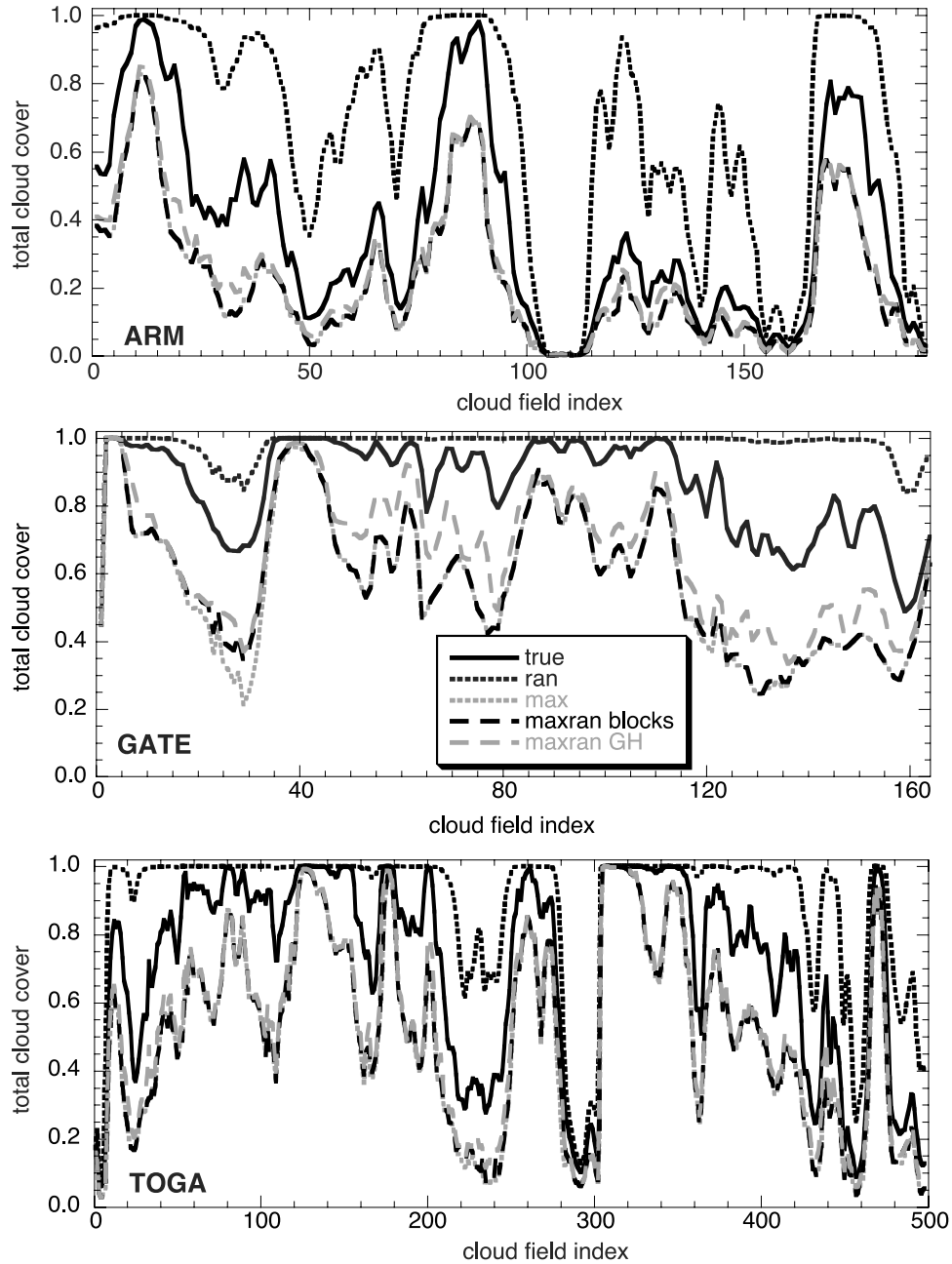

Figure 3. Total cloud cover of each (512 km)^2 domain cloud field as estimated from the number of cloudy columns (“true”) and as calculated from layer cloud fractions using the random (“ran”), maximum (“max”) and two maximum/random overlap assumptions (“maxran blocks” and “maxran GH”). See text for details.

Table 1. Total Cloud Cover RMS Errors for the Various Overlap Approximations[a]

	Ran (512 km)^2	Max (512 km)^2	Maxran1 (512 km)^2	Maxran2 (512 km)^2	Ran (256 km)^2	Max (256 km)^2	Maxran1 (256 km)^2	Maxran2 (256 km)^2
ARM	0.350	0.190	0.190	0.165	0.289	0.175	0.172	0.144
GATE	0.167	0.308	0.296	0.221	0.164	0.298	0.281	0.200
TOGA	0.233	0.233	0.223	0.203	0.215	0.224	0.217	0.186

[a]Here “maxran1” is “maxran blocks” and “maxran2” is “maxran GH” of Figure 3.

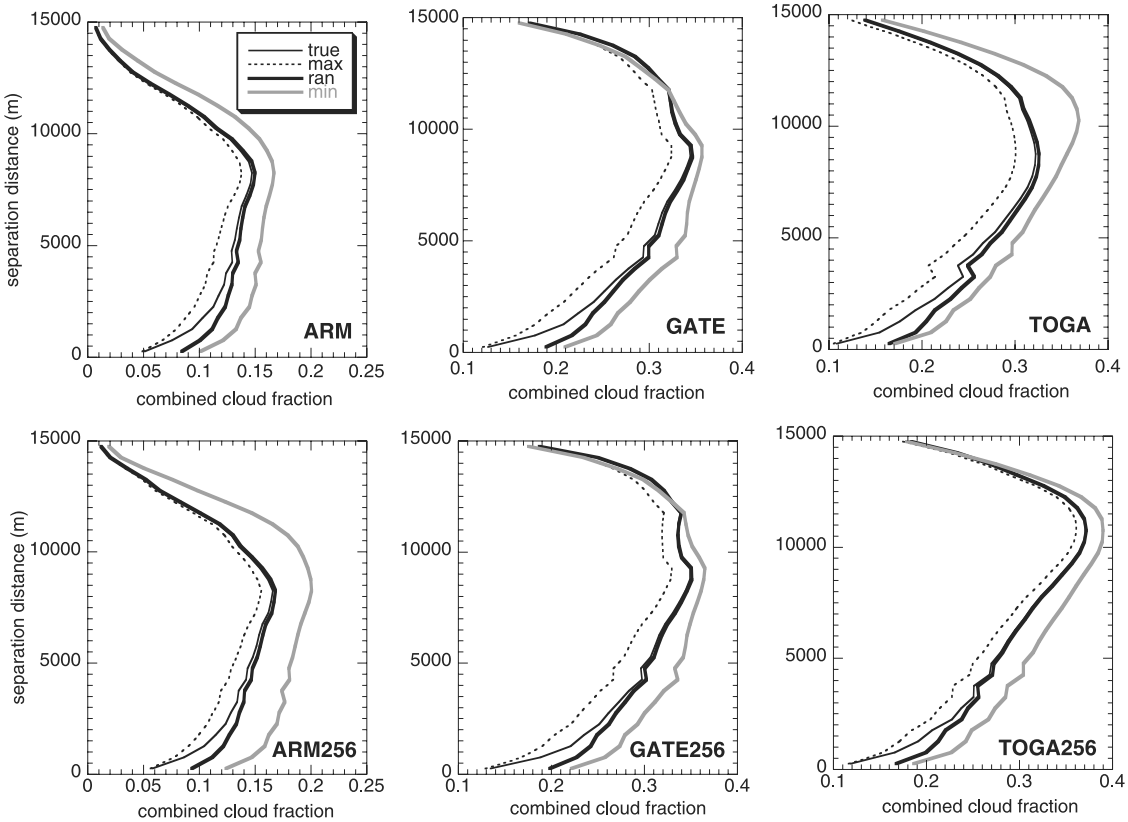

Figure 4. Ensemble average of combined cloud fraction of pairs of layers separated vertically by distances shown in the ordinate as "observed" from the modeled fields ("true") and as derived using the maximum ("max"), random ("ran"), and minimum ("min") overlap assumptions. Top row is for analysis of the entire (512 km)^2 domain while bottom row is for analysis of (256 km)^2 subdomains.

which are, respectively, the cloud fractions corresponding to the maximum, minimum, and random overlap assumption. The true combined cloud fraction of two cloud layers most often does not agree with any of the cloud fractions derived from (1). HI2000 introduced a parameter α to quantify the degree of agreement between the combined true cloud fraction C_{true} and that from the overlap assumptions:

$$C_{\text{true}} = \alpha\, C_{\text{max}} + (1-\alpha) C_{\text{ran}} \tag{2}$$

According to the above formulation, $\alpha = 0$ corresponds to random overlap, $\alpha = 1$ to maximum overlap, while negative values of α indicate cloud fractions larger than C_{ran} that start approaching values of C_{min} (MBT2002).

[10] Figure 3 shows the total cloud cover for each cloud field. Five different estimates are shown. "True" is the actual total cloud cover, as "observed". It is estimated as the fraction of the total number of columns that are cloudy. A column is considered cloudy if it contains one or more cloudy grid boxes. The "max" curve corresponds to the total cloud cover using the maximum overlap assumption (generalization of equation (1a) for multiple cloud layers) and is simply equal to the maximum cloud fraction of the vertical profile. The "ran" curve corresponds to the total cloud cover from the random overlap assumption and is derived from a generalization of equation (1c) for multiple (N) cloud layers:

$$C_{\text{ran}} = 1 - \prod_{i=1}^{N} (1 - C_{\text{i}}) \tag{3}$$

The "maxran blocks" curve is derived by combining the maximum and random overlap assumption in the following way: contiguous cloud layers form blocks; whenever a clear layer exists a new cloud block is formed; the cloudy layers within a block overlap according to the maximum overlap assumption, while cloud blocks themselves overlap according to the random overlap assumption. Thus equation (3) is used with N being the number of cloud blocks and each C_{i} representing the maximum cloud fraction within the block. Finally, the curve "maxran GH" is the total cloud cover according to the combined maximum/random overlap assumption as implemented by *Geleyn and Hollingsworth* [1979]:

$$C_{\text{maxran}} = 1 - (1 - C_1) \times \prod_{i=2}^{N} \frac{1 - \max(C_{\text{i}-1}, C_{\text{i}})}{1 - C_{\text{i}-1}} \tag{4}$$

The *Geleyn and Hollingsworth* [1979] implementation of maximum/random overlap differs from the "block"

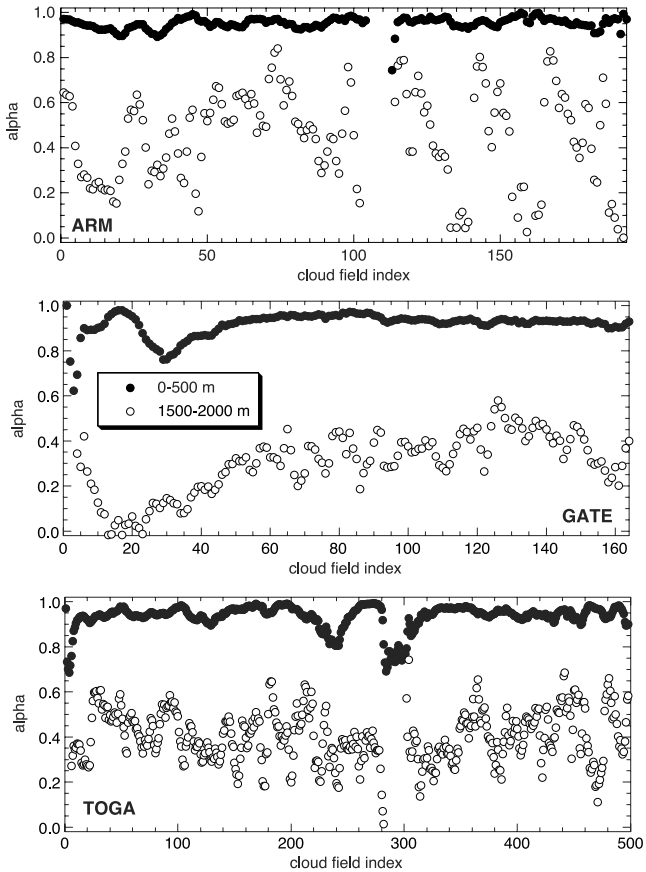

Figure 5. Values of α for all $(512\ \text{km})^2$ domain cloud fields derived from the true combined cloud fraction and the combined cloud fraction of the random, and maximum overlap assumption using equation (2). Pairs of layers separated by distances either within the 0–500 m range or the 1500–2000 m range are shown.

approach in that layers within a block are considered maximally overlapped only when there is no local cloud fraction minimum in between. Thus the Geleyn and Hollingsworth method generally results in a larger cloud cover than the "block" method.

[11] For the CRM fields, the true total cloud cover assumes values between those derived from the random and maximum overlap assumptions. In addition, neither of the two max/ran overlap assumptions is a particularly good fit. The "block" max/ran scheme gives values almost identical to the maximum overlap scheme for all three sets of runs. The reason is that for the majority of fields, clouds form a single block, i.e., clouds are contiguous. For the GATE fields, equation (4) performs better than the maximum overlap assumption, but still underestimates substantially the true total cloud cover. These results are also summarized in Table 1 as total cloud cover RMS errors of the various approximations. It can be seen that for $(256\ \text{km})^2$ domain size performance is slightly improved.

[12] Figure 4 shows the ensemble-average (i.e., averaged over all snapshots) combined cloud fraction of two cloudy layers as a function of their vertical separation distance Δz shown in the ordinate. The true combined cloud fraction is compared with combined cloud fraction derived from the maximum, random, and minimum overlap assumptions. The vertical separation bin size is 500 m. Figure 4 is similar to Figure 3 of HI2000 and panel a of Figures 3–5 of MBT2002. Note, however, that in contrast to their work, we do not distinguish between pairs of layers with and without cloud in the intervening layers. The reason is that in the majority of cases only one cloud block is present (recall the small difference between "max" and "maxran blocks" cloud fraction in Figure 3), so that statistics for the rare occurrences of layers separated by clear skies are quite limited and applicable only to the case of large separation distances. As expected, the true combined cloud fraction of the pair lies between its counterparts for the random and maximum overlap assumption. For small separation distances (first two bins, $\Delta z < 1000$ m) the two layers overlap in a manner resembling maximum overlap conditions, but very quickly true combined cloud fraction takes values

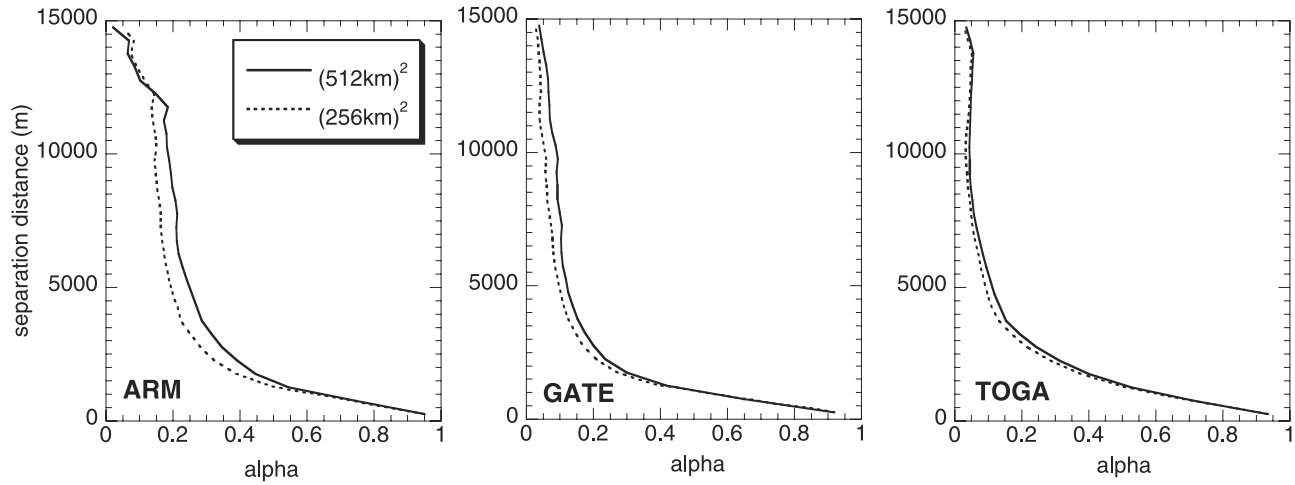

Figure 6. Ensemble average profiles of α derived for the original $(512\ \text{km})^2$ domain and for $(256\ \text{km})^2$ subdomains.

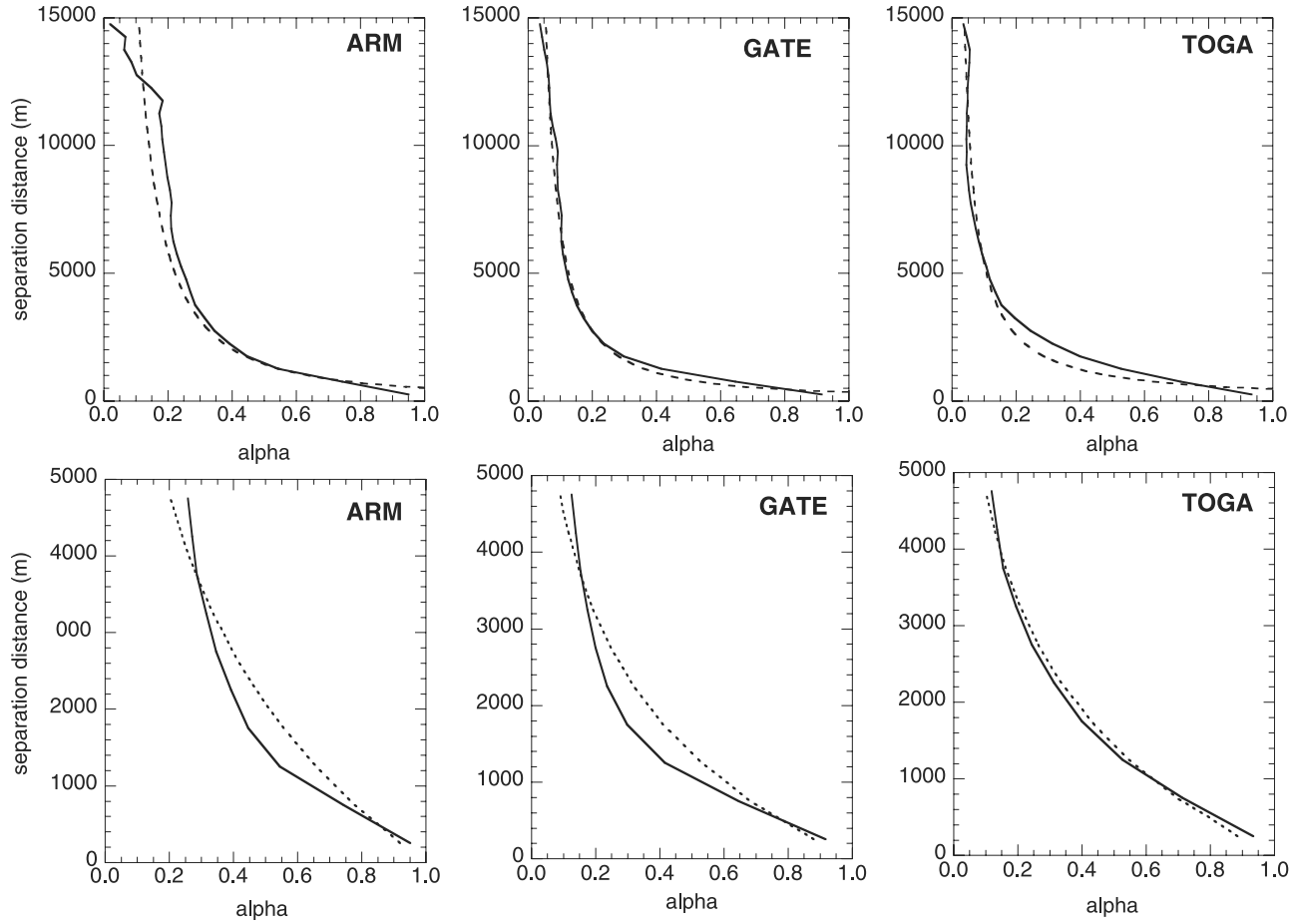

Figure 7. Power law fits (equation (5a)) of the ensemble averaged α for vertical separation distances up to 15 km (top row, dashed curve) and exponential fits (equation (5b)) for separation distances up to 5 km (bottom row, dashed curve). The solid curves are the original ensemble average profiles of α.

between those for maximum and random overlap. Conditions of almost purely random overlap prevail when the layers are separated by more than 5 km. However, it would probably not be wise to attempt to incorporate directly into radiative transfer calculations overlap effects of clouds too far apart, unless, of course, only clear skies separate the two distant layers. When some of the intervening layers are cloudy, radiative interactions are already so complex that details of the overlap of two remote layers will usually have small effect on the radiative flux profile.

[13] There are slight increases in the combined cloud fractions when the analysis is performed for the $(256\ \text{km})^2$ domains. This means that the degree of overlap decreases when the domain size becomes smaller. This is consistent with the findings of HI2000 who noted that as the temporal scale over which they were sampling MMCR data increased (effectively larger spatial domains) so did the overlap.

[14] Figure 5 shows individual values of α derived from equation (2), and averaged for each snapshot, for pairs of layers separated by distances either within the 0–500 m range or the 1500–2000 m range (i.e., first and fourth Δz bin in our analysis). The values for the first bin are not much variable and are close to the value that corresponds to the maximum overlap assumption ($\alpha = 1$), as expected. In contrast, the α values for the fourth bin have a significant degree of variability and indicate that in some occasions random overlap conditions have already been established when the cloud layers are separated by $\Delta z \sim 2$ km. In general, as Δz increases, so does the variability of α and the number of snapshots for which combined cloud fractions can no longer be calculated because of unavailability of clouds in one of the two layers.

[15] Figure 6 shows ensemble-average profiles of α. There are two curves for each of the ARM, GATE, and

Table 2. Least Squares Fit Parameters and Correlation Coefficients for Equation (5a)

	c (512 km)^2	b (512 km)^2	R (512 km)^2	c (256 km)^2	b (256 km)^2	R (256 km)^2
ARM	56.1	0.65	0.944	37.2	0.62	0.970
GATE	78.3	0.75	0.970	196.9	0.89	0.954
TOGA	299.1	0.93	0.906	370.6	0.97	0.905

Table 3. Δz_0 and Correlation Coefficient From Least Squares Fitting Equation (5b) for Separation Distances Less Than 5 km

	Δz_0 (512 km)^2, m	R (512 km)^2	Δz_0 (256 km)^2, m	R (256 km)^2
ARM	2990	0.969	2526	0.972
GATE	1971	0.976	1799	0.980
TOGA	2068	0.997	1914	0.997

TOGA cloud fields corresponding to the two domain sizes used in our analysis, As expected, α drops with separation distance, indicating that as cloud layers become more distant they acquire an increasingly stronger tendency for random overlap. This tendency is slightly more pronounced for the smaller domain size, especially for the ARM data set.

[16] Figure 7, top row, shows least squares power fits to the solid curves of Figure 6 (large domains). The parameters of the power law function

$$\alpha = c\Delta z^{-b} \tag{5a}$$

and the goodness of fit coefficient R are given in Table 2 for both domain sizes. The least successful power law fit is for the TOGA data set. However, the power law function is not very suitable for LSM parameterization purposes since it does not have the required property that $\alpha \rightarrow 1$ as $\Delta z \rightarrow 0$. A function that has this property is the exponential function proposed by HI2000:

$$\alpha = \exp(-\Delta z/\Delta z_0) \tag{5b}$$

Δz_0 has now the physical meaning of the e-folding or "decorrelation" distance (HI2000). The exponential fit does not perform very well when applied to the entire range of separation distances, but when restricted to a maximum separation distance of 5 km, which would be of most importance in modeling applications, the quality of fit is quite good (Figure 7, bottom row, and Table 3). The results in Table 3 suggest an increase in Δz_0 for an increase in domain size, in agreement with similar results by HI2000.

[17] Provided that fits of this type can be reproduced from more data sets, one can envision the introduction in an LSM of a completely generalized overlap scheme where the combined cloud fraction of any two layers is given by equation (2) with α values provided as a function of separation distance from parameterizations such as equation (5b). A solar radiative transfer algorithm based on this concept was presented by *Bergman and Rasch* [2002].

4. Discussion and Conclusions

[18] We have shown that the overlap properties of numerous convective cloud fields generated by a CRM show consistency with previous analyses from ground-based millimeter radar data (HI2000; MBT2002). We reach this conclusion using spatial cloud variability. We did not attempt to emulate MMCR-type cloud observations by following the temporal evolution of selected cloudy columns drawn from our CRM "snapshots" as by *Barker et al.* [1999b] because of the coarse temporal sampling (1 hour) and the rapid decorrelation of our cloud fields.

[19] We found that the total cloud cover and the combined cloud fraction of any two layers separated by a certain distance assumes values between those corresponding to the maximum and random overlap assumptions. The value of the parameter α describing the degree to which cloud fraction agrees with the idealized overlap assumptions is a smooth varying function of separation distance and can be fit with analytical functions. This may turn out to be very useful for parameterization purposes. An added advantage of the type of overlap scheme presented in this work, as well as in those of HI2000 and MBT2002 is that it does not parameterize cloud overlap based on which layers are cloudy, but on the vertical separation of cloudy layers expressed in physical units of distance. Such an overlap scheme, does not explicitly depend on details of the vertical discretization, and is therefore not very sensitive to changes in vertical resolution [*Bergman and Rasch*, 2002]. Random and maximum/random overlap schemes, in contrast, can be very sensitive to the details of vertical discretization.

[20] Overlap analysis such as this presented in the current study should continuously be extended with results for other cloud types and ultimately be considered for implementation in the radiative transfer schemes of LSMs or even stochastic multilayer cloud generators. Efforts have already begun in this direction [*Bergman and Rasch*, 2002; *Oreopoulos et al.*, 2002], despite the inherent difficulties in conveying the overlap information into the radiation algorithm in a meaningful way. Things become even more complex when attempting to account not only for cloud overlap, but also concurrently for horizontal inhomogeneity, and vertical correlations of cloud water [*Hogan and Illingworth*, 2003]. Nonetheless, initial evidence suggests that even at their current stage of development these algorithms are capable of outperforming current plane-parallel algorithms with standard overlap assumptions.

[21] **Acknowledgments.** This research was supported by the Office of Biological and Environmental Research of the U. S. Department of Energy (under grant DE-AI02-00ER62939) as part of the Atmospheric Radiation Measurement Program, and NASA grant NAG5-11631. We benefited from discussions with H. W. Barker and P. Räisänen. The comments of two anonymous reviewers greatly helped to improve the paper.

References

Barker, H. W., G. L. Stephens, and Q. Fu, The sensitivity of domain-averaged solar fluxes to assumptions about cloud geometry, *Q. J. R. Meteorol. Soc.*, *125*, 2127–2152, 1999a.

Barker, H. W., E. E. Clothiaux, T. P. Ackerman, R. T. Marchand, Z. Li, and Q. Fu, Overlapping cloud: What radars give and what models require, paper presented at 9th ARM Science Team Meeting, Atmos. Radiat. Meas. Program, San Antonio, Tex., 1999b.

Barker, H. W., et al., Assessing 1D atmospheric solar radiative transfer models: interpretation and handling of unresolved clouds, *J. Clim.*, in press, 2003.

Bergman, J. W., and P. J. Rasch, Parameterizing vertically coherent cloud distributions, *J. Atmos. Sci.*, *59*, 2165–2182, 2002.

Geleyn, J. F., and A. Hollingsworth, An economical analytical method for the computation of the interaction between scattering and line absorption of radiation, *Contrib. Atmos. Phys.*, *52*, 1–16, 1979.

Hogan, R. J., and A. J. Illingworth, Deriving cloud overlap statistics from radar, *Q. J. R. Meteorol. Soc.*, *126*, 2903–2909, 2000.

Hogan, R. J., and A. J. Illingworth, Parameterizing ice cloud inhomogeneity and the overlap of inhomogeneities using cloud radar data, *J. Atmos. Sci.*, *60*, 756–767, 2003.

Khairoutdinov, M. F., and D. A. Randall, Cloud resolving modeling of the ARM Summer 1997 IOP: Model formulation, results, uncertainties and sensitivities, *J. Atmos. Sci.*, *60*, 607–625, 2003.

Mace, G. G., and S. Benson-Troth, Cloud layer overlap characteristics derived from long-term cloud radar data, *J. Clim.*, *15*, 2505–2515, 2002.

Oreopoulos, L., and H. W. Barker, Accounting for subgrid-scale cloud variability in a multi-layer 1D solar radiative transfer algorithm, *Q. J. R. Meteorol. Soc.*, *126*, 301–330, 1999.

Oreopoulos, L., H. W. Barker, M.-D. Chou, R. F. Cahalan, and M. Khairoutdinov, Allowing for inhomogeneous clouds in the Goddard Earth Observing System GCM Column Radiation Model, paper presented at 11th Conference on Atmospheric Radiation, Am. Meteorol. Soc., Ogden, Utah, 2002.

Stephens, G. L., et al., The CloudSat mission and the A-Train: A new dimension of space-based observations of clouds and precipitation, *Bull. Am. Meteorol. Soc.*, *83*, 1771–1790, 2002.

Tian, L., and J. A. Curry, Cloud overlap statistics, *J. Geophys. Res.*, *94*, 9925–9935, 1989.

L. Oreopoulos, Joint Center for Earth Systems Technology, University of Maryland Baltimore County, 1000 Hilltop Circle, Baltimore, MD 21250, USA. (lazaros@climate.gsfc.nasa.gov)

M. Khairoutdinov, Department of Atmospheric Sciences, Colorado State University, Fort Collins, CO 80523, USA.